

The chemical content of a sample of dwarf irregular galaxies^{*}

A. M. Hidalgo-Gómez^{**} and K. Olofsson

Astronomiska observatoriet, Box 515, 751 20 Uppsala, Sweden
e-mail: kjell.olofsson@astro.uu.se

Received 7 August 2001 / Accepted 29 April 2002

Abstract. We present abundances of neon, nitrogen and oxygen of some nearby dwarf irregular galaxies. The elemental abundances are retrieved from long-slit spectroscopy of H II regions in the objects. The abundances are found to be sub-solar in all cases. For the dwarf irregular galaxy DDO 190 the abundances reported in this work are the first ever published. One object, DDO 167, proved to have an oxygen abundance about similar to the one of I Zw 18, even though the uncertainties are high. A comparison of the chemical abundances between all the groups of gas-rich galaxies have been performed and the main conclusion is that the dwarf gas-rich galaxies are not distinguishable on the basis of their chemical content.

Key words. galaxies: evolution – galaxies: irregular – galaxies: stellar content – galaxies: dwarf

1. Introduction

Studies of galaxies with very low metallicities, such as I Zw 18 (Kunth & Sargent 1986) and SBS 0335-052 (Thuan et al. 1997), could shed some light on the formation of galaxies in general. The search for such extremely low metallicity galaxies is one of the hot topics in astronomy today. More chemically evolved galaxies, with oxygen abundances in the range of $7.4 \leq 12 + \log(\text{O}/\text{H}) \leq 8.3$, could make the connection between these quasi-primordial systems and normal galaxies. Star-forming galaxies are candidates for such a group of intermediate galaxies, especially dwarf and magellanic irregular galaxies. The chemical abundances of a sample of dwarf irregular (dI) galaxies, IC 5152, DDO 168, DDO 167, Gr 8 and DDO 190, are reported in this investigation.

The galaxies were selected from the sample of Hidalgo-Gómez & Olofsson (1998) (hereafter; HGO). In all cases, several H II regions were detected from H α images which made them excellent candidates for a more detailed analysis of their chemical composition.

IC 5152 is an isolated galaxy outside the Local Group at a distance of 1.7 Mpc (Zijlstra & Minniti 1999). Two determinations of the chemical abundances of IC 5152 exist (Talent 1980; Webster et al. 1983). They gave very

similar results although both sets of data are old (from the early eighties) and the chemical abundance of one of them was determined from empirical metallicity calibrations. A study of the stellar content of IC 5152 has been carried out fairly recently (Zijlstra & Minniti 1999). The central region of this galaxy is an active site of star formation, with a substantial amount of young stars.

DDO 190 is an isolated galaxy. The distance has been measured recently with the aid of the tip of the red giant branch (Aparicio & Tikhonov 2000) and was estimated to be $2.9 \pm .2$ Mpc. This distance is shorter than previous estimations. No estimate of the metallicity of DDO 190 has been reported previously. The H α image obtained by the authors reveals several prominent H II regions, which makes this galaxy interesting for a more detailed study.

DDO 167 is a small galaxy with several, mostly faint, H II regions. The chemical abundance was determined by Skillman et al. (1989), obtaining a low value for the oxygen abundance, although the quality of the spectrum was poor.

DDO 168 is a large, isolated galaxy at a distance of 4.2 Mpc (HGO). DDO 168 was classified as a Ir IV-V by van den Bergh (1966) and reveals very blue broadband colours (Gallagher & Hunter 1986). From a recent broadband photometric study of this galaxy (Schulte-Ladbeck & Hopp 1998) was concluded that a significant fraction of stellar mass was produced in the recent history of the object. However, Hunter & Hoffman (1999) obtained a very high value of the oxygen abundance of this galaxy based on the empirical method.

Gr 8 is a very well-known nearby galaxy dominated by two large and bright H II regions denoted Hodge 1 and 2.

Send offprint requests to: A. M. Hidalgo-Gómez,
e-mail: anamaria@astro.uu.se

^{*} Based on observations made at the European Southern Observatory, La Silla, Chile, the Nordic Optical Telescope, La Palma, Spain, and Calar Alto Observatory, Almería, Spain.

^{**} *Present address:* Instituto Politécnico Nacional, Mexico city, Mexico; e-mail: ana@esfm.ipn.mx

Table 1. The log of the observations. The identification of the object and the coordinates are shown in Cols. 1 to 3. Columns 4, 5 and 6 give the date of observation, the telescope and instrument used. The position angle is found in Col. 7 while the integration time and air masses are in given in Cols. 8 and 9, respectively. The seeing is presented in the last column.

Galaxy	α	δ	Date	Telescope	Instrument	Pos. Angle	Int. Time blue/red	Air Mass blue/red	seeing
IC 5152	22 02 41.9	-51 17 44	110897	3.6 m LS	EFOSC 1	327	90/50	1.15/1.37	1.3''
DDO 190	14 24 43.4	44 31 33	190498	NOT	ALFOSC	216	60/50	1.1/1.2	1''
DDO 167	13 13 22.7	46 19 13	200498	NOT	ALFOSC	198	30/-	1.05/-	1''
DDO 168	13 14 27.9	45 55 09	200498	NOT	ALFOSC	198	60/50	1.32/1.4	1''
Gr 8	12 58 40	14 13 00	240398	3.5 m CAHA	TWIN	303	75	1.5	

Its extremely blue colour, $(B - V) = 0.26$ (Gallagher & Hunter 1986) and its active star formation (Dohm-Palmer et al. 1998) make it a perfect candidate for this investigation. Moreover, in previous determinations, the oxygen abundance varied largely from author to author. The recent star formation has been recently studied by Dohm-Palmer et al. (1998). They found a constancy on the star formation rate during the past 500 Myr.

Section 2 presents the observations and reductions of the data. The analysis, with details on the uncertainties and extinction corrections, is presented in Sect. 3. The results on the spatially-averaged chemical abundances are given in Sect. 4, and Sect. 5 presents a discussion on the chemical evolution of dIs and its connection with the other types of gas-rich galaxies. Finally, conclusions are given in Sect. 6.

2. Observations and data reductions

The galaxies presented have been observed with different telescopes and detector configurations from August 1997 to April 1998. A log of the observations is presented in Table 1.

Spectra of IC 5152 were obtained with the use of the ESO (European Southern Observatory) 3.6 m telescope at La Silla, Chile, with EFOSC1 on the 10th of August of 1997. The H_α image, obtained as an aid for positioning the slit, revealed a few small H II regions towards the western part of the galaxy. Since no nebular emission was detected in the main body, where instead Balmer lines in absorption were prominent, spectroscopy of these small regions was performed. The slit was oriented in the SE-NW direction passing through four H II regions at a position angle of 327° . The emission line $[\text{OIII}]\lambda 4363 \text{ \AA}$ was detected in only one of them. Due to the large pixel size of EFOSC1 no correction for differential refraction was performed (see Hidalgo-Gómez et al. 2001a, hereafter Paper I, for details).

The galaxies DDO 167, DDO 168 and DDO 190 were observed with the 2.5 m Nordic Optical Telescope, (NOT) at La Palma, Canary Islands, on the 19:th and 20:th of April 1998. The instrumentation used was ALFOSC and the Loral CCD with a pixel size of $15 \mu\text{m}$ and a FOV of $6'.5 \times 6'.5$. The nominal resolution of the configuration was 4 \AA . Two slit positions were used for DDO 190, one passing through regions denoted 2 and 6 in

Aparicio & Tikhonov (2000) and the second one through regions denoted 3 and 8. The line $[\text{OIII}]\lambda 4363 \text{ \AA}$ was only detected with confidence in region 3. Only one slit position is presented for DDO 167. It passed through the region No. 8 (Strobel et al. 1990), the sole H II region in which the oxygen line $[\text{OIII}]\lambda 4363 \text{ \AA}$ was detected. Two slit positions were chosen for DDO 168, both passing through the main chain of H II regions observed in this galaxy (Strobel et al. 1990). Their orientations were mutually parallel, and only in a single H II region the oxygen line $[\text{OIII}]\lambda 4363 \text{ \AA}$ was detected. For all three galaxies, corrections due to differential diffraction were performed, despite the low air masses, due to the small pixel size of the CCD ($0.19''$ per pixel).

Gr 8 was observed with the 3.5 m telescope at the Calar Alto Observatory (Almería, Spain) on the 24th of March 1998. The spectrograph TWIN was used in the observations as well as the CCD 6a (blue) and 4a (red), both each of 800×2000 pixels. The gratings were T08 and T04 covering a total range in wavelength between 3500 \AA and 7870 \AA . The dispersion of both gratings was 72 \AA/mm . The night was mostly clear. Two slit positions were obtained, both encompassing the two main H II regions Hodge 1 and 2, but the oxygen line $[\text{OIII}]\lambda 4363 \text{ \AA}$ was detected, with confidence, only at some parts of Hodge 2. The air masses were high, up to 1.5, and corrections for differential refraction were performed.

Data were reduced with the software package MIDAS as described in Paper I. Different standard stars were chosen for the flux calibration. The accuracy of such calibrations was 5% in the blue and 8% in the red for the data on IC 5152, 1% and 3% for DDO 167, DDO 168 and DDO 190 and 13% for Gr 8. The blue and red parts of the spectrum of IC 5152 were not perfectly aligned. Therefore the lines in the red part of the spectrum were normalized to the H_α line intensity (see Hidalgo-Gómez et al. 2001b for details). Gr 8 presented a more complicated situation. A mercury sky line was located between H_γ and the oxygen line $[\text{OIII}]\lambda 4363 \text{ \AA}$. In order to retrieve the intensity of $[\text{OIII}]\lambda 4363 \text{ \AA}$, it was decided not to perform the sky subtraction since the oxygen line resided on the shoulder of the Hg line. A gaussian profile was fitted to the Hg line for all the H II regions observed and the residual intensity from the average value was regarded as the $[\text{OIII}]\lambda 4363 \text{ \AA}$ line intensity.

A spectrum for each H II region was obtained by adding all rows where the oxygen line [OIII] λ 4363 Å was detected. The total number of rows were 6 for IC 5152, 42 for Gr 8, 13 for DDO 167, 5 for DDO 168 and 10 for DDO 190. The intensity of the spectral lines was measured with software developed at the Uppsala Astronomical Observatory (see Paper I for details).

3. Analysis of the data

3.1. Errors in the continuum and line intensities

The determination of the uncertainties in the spectral line intensities and continuum becomes of the utmost importance when the signal-to-noise ratio is low, which is the case for some of the data presented in this analysis. Three major sources of uncertainties have been considered in this investigation, as described in Paper I and Hidalgo-Gómez et al. (2001b; hereafter Paper II) For spectra with the lowest signal-to-noise ratios the total uncertainty, obtained as the sum of each of these terms, is very high especially for [OIII] λ 4363 Å. For spectra with medium signal-to-noise ratio (such as those of IC 5152 and DDO 190) the major contributor to the uncertainty is the continuum level determination, which is lower than 15% in the oxygen line [OIII] λ 4363 Å. Another 10% is due to the extinction correction. For DDO 167 the uncertainty due to the continuum level determination is as high as 70%. A similar value is obtained for DDO 168. Due to the difficulties in the determination of the [OIII] λ 4363 Å line intensity for Gr 8 (see Sect. 2), a total uncertainty of 50% should be considered for this line due to the continuum level determination.

3.2. The correction for underlying stellar absorption and extinction

The line intensities obtained were corrected for extinction and underlying stellar absorption as described in Paper I. Extinction coefficients were obtained for all the H II regions observed which is useful in order to retrieve information about the distribution of dust towards these galaxies.

Due to a difference of less than one pixel between the blue and red part of the spectrum of IC 5152, the intensities in the red part were normalized to the H α emission line and the extinction coefficient, C_β , was derived with the aid of the H γ line (see Paper II for details). In the spectra of IC 5152, DDO 168 and DDO 190 several Balmer lines are present and C_β could be determined from each of these. The corresponding values are presented at the end of Table 2. The C_β coefficient were determined in three out of the six H II regions observed in IC 5152. The southeastern region may have a lower dust content than those towards the north, which might be indicative of a clumpy distribution of dust. For DDO 190, the two values in the C_β are consistent and very similar. On the contrary, the two C_β values of DDO 168 show large differences.

4. The spatially-averaged chemical abundances

Table 2 also presents the intensity of the spectral lines, the equivalent width and flux of the H β emission line as well as the signal-to-noise ratio in the line [OIII] λ 4363 Å of each dI. The abundance of the chemical elements was derived from the intensity of the spectral lines as described in Papers I and II. The physical parameters derived from them are presented in Table 3 as well as the temperature of the ionizing radiation, T_{ion} . The latter was derived as in Olofsson (1997).

4.1. A Supernova in IC 5152?

Some spectral characteristics need to be commented on. Perhaps the most important characteristic in the spectrum of IC 5152 is the line HeII λ 4686 Å. It is a feature indicative of, either, a very hot stellar population, which provides very energetic photons which photoionize the nebula (e.g. Osterbrock 1989), or could be due to Wolf-Rayet (WR) stars (Aller 1984). Another possibility to consider is the existence of a SN type II (Masegosa 1998). The absence of nebular lines such as [ArIV] λ 4471 Å rules out a nebular origin for the He II line in spite of the large spatial coverage, 26 pc, which is not indicative of a stellar origin. The high equivalent width of the feature, 13 Å, as well as the detection of the [OI] λ 6300, 6363 doublet, which could be an indication of strong winds, are evidences in favour of this stellar origin. The caveats are the large uncertainties associated with the [OI] doublet (more than 50%) and the fact that the intensity of the feature is explained by photoionization only (Stasińska 1990). On the other hand, it is very striking the absence of other WR features, especially the typical “red bump” between 5700 and 5800 Å. Other important features that appear in the spectrum when WR stars are presented, like [Fe III] λ 4658 Å or [CIV] λ 4658 Å are not clearly detected, but they could be blended with the He II line due to its broadness. Although a WR origin can not be completely ruled out, the SN origin must be also considered. If this were the case, an overabundance of oxygen and neon may be expected. From Table 3, it is noted that the spectrum of IC 5152 has a relatively high abundance of both elements lending support to the SN origin. On the contrary, as evident from Fig. 1, IC 5152 does not deviate significantly compared to the rest of the sample despite the WR feature in the spectrum. In conclusion, the He II lines detected in the spectrum of IC 5152 have likely an stellar origin, but the distinction between a WR star and a SN type II needs a more detailed analysis.

4.2. Comparison with previous work

Our data on DDO 167, DDO 168 and Gr 8 are of quite low quality. The quality of the data on DDO 167 in Skillman et al. (1989) is similar to the present data, but large differences are found between both determinations ($12 + \log(\text{O}/\text{H}) = 7.66$ compared with the value

Table 2. Line intensities of the spatially-averaged spectra, normalized to H_β , of the H II regions studied in this investigation. The last three lines correspond to the equivalent width of H_β , $E_v(H_\beta)$, the flux in the H_β line, $F(H_\beta)$, as well as the signal-to-noise ratio in the line $[OIII]\lambda 4363 \text{ \AA}$, $\sigma(l)_{4363}$. Also, the extinction coefficient, C_β , derived from the non-corrected Balmer lines intensities, are presented.

line	λ (Å)	IC 5152	DDO 190	DDO 167	DDO 168	Gr 8
[OII]	3727	4 ± 3	3 ± 2	1 ± 1	$1.9 \pm .9$	$1.6 \pm .8$
H10	3798	-	$0.08 \pm .08$	-	-	-
H9	3835	-	$0.1 \pm .1$	-	-	-
[NeIII]	3869	$0.7 \pm .5$	$0.6 \pm .4$	-	$0.13 \pm .07$	-
HeI	3889	$0.1 \pm .1$	$0.3 \pm .2$	-	-	-
[NeIII]	3967	$0.3 \pm .2$	$0.4 \pm .3$	-	$0.1 \pm .1$	-
H δ	4102	$0.28 \pm .05$	$0.4 \pm .3$	-	$0.07 \pm .05$	-
H γ	4340	$0.469 \pm .1$	$0.57 \pm .1$	$0.469 \pm .6$	$0.2 \pm .1$	$0.469 \pm .1$
[OIII]	4363	$0.07 \pm .03$	$0.07 \pm .02$	$0.3 \pm .4$	$0.05 \pm .1$	$0.04 \pm .01$
HeI	4471	$0.07 \pm .03$	$0.04 \pm .01$	-	-	$0.08 \pm .05$
HeII	4650	$0.36 \pm .04$	-	-	-	-
H β	4861	$1.00 \pm .01$	$1.00 \pm .06$	$1.00 \pm .06$	$1.0 \pm .1$	$1.00 \pm .02$
[OIII]	4959	$1.9 \pm .1$	$1.4 \pm .1$	$1.01 \pm .1$	$0.6 \pm .1$	$0.53 \pm .02$
[OIII]	5007	$5.7 \pm .4$	$4.4 \pm .2$	$3.1 \pm .2$	$2.0 \pm .1$	$1.586 \pm .004$
HeI	5875	$0.101 \pm .004$	-	-	-	-
[OI]	6300	0.005 ± 0.005	-	-	-	-
[SIII]	6312	$.009 \pm .003$	-	-	-	-
[OI]	6363	$0.015 \pm .01$	-	-	-	-
[NII]	6548	$0.02 \pm .01$	$0.01 \pm .01$	-	-	-
H α	6563	$1.3 \pm .1$	$2.86 \pm .8$	-	$2.86 \pm .1$	-
[NII]	6583	$0.10 \pm .02$	$0.04 \pm .02$	-	-	-
HeI	6678	$0.019 \pm .004$	$0.07 \pm .04$	-	-	-
[SII]	6716	$0.14 \pm .04$	$0.26 \pm .1$	-	-	-
[SII]	6730	$0.10 \pm .03$	$0.21 \pm .1$	-	-	-
$E_v(H_\beta)\text{\AA}$		14	128	70	32	11
$\log F(H_\beta)$		-13.21	-12.48	-14.29	-14.65	-12.58
$\sigma(l)_{4363}$		4.2	1.0	-	-	-
$C_\beta(H\alpha)$		-	$3.01 \pm .08$	-	$2.5 \pm .2$	-
$C_\beta(H\gamma)$		1.76	0.99	1.5 ± 2	2.57	$0.7 \pm .7$
$C_\beta(H\delta)$		1.4	0.53	-	5.78	-
$C_\beta(H9)$		1.16	-	-	-	-
$C_\beta(H10)$		1.27	-	-	-	-

Table 3. Physical parameters for the H II regions in the dIs of the present study. The electron temperature, $T_e(O^{++})$, for DDO 167 is an upper limit, therefore, the oxygen abundance must be interpreted as a lower limit. T_{ion} is the temperature of the ionizing radiation. The abundance of various elements are given as well as their ICFs. The bottom row refers to a determination of the oxygen abundance with the use of the semi-empirical method (McGaugh 1994).

line	IC 5152	DDO 190	DDO 167	DDO 168	Gr 8
$T_e(O^{++})$	$12\,300 \pm 1500 \text{ K}$	$13\,900 \pm 1100 \text{ K}$		$18\,000 \pm 15\,000 \text{ K}$	$18\,100 \pm 5000 \text{ K}$
T_{ion}	50 000 K	-	46 865 K	42 271 K	42 668 K
$12 + \log(O/H)$	$8.2 \pm .1$	$8.01 \pm .03$	$7.2 \pm .2$	$7.5 \pm .2$	$7.4 \pm .1$
ICF(N)	$2.8 \pm .4$	$2.5 \pm .8$	-	-	-
$12 + \log(N/H)$	$6.48 \pm .1$	$5.97 \pm .1$	-	-	-
$\log(N/O)$	$-1.7 \pm .1$	$-2.0 \pm .1$	-	-	-
ICF(Ne)	$1.5 \pm .1$	$1.66 \pm .1$	-	2 ± 4	-
$12 + \log(Ne/H)$	$7.7 \pm .1$	$7.6 \pm .1$	-	$6.8 \pm .7$	-
$\log(Ne/O)$	$-0.5 \pm .1$	$-0.41 \pm .1$	-	$-0.69 \pm .02$	-
$N(He)/N(H)$	$0.09 \pm .03$	$0.2 \pm .1$	-	-	-
$12 + \log(O/H)_{sem}$	-	8.27	7.8	7.76	7.6

of 7.2 presented here). Concerning Gr 8, the data presented here indicate a low oxygen abundance, closer to the one derived by Skillman et al. (1988) [$12 + \log(\text{O}/\text{H}) = 7.45$] than the value obtained by Moles et al. (1990) [$12 + \log(\text{O}/\text{H}) = 7.66$].

Extremely large differences are found between the value of the oxygen content in DDO 168 by Hunter & Hoffman (1999), $12 + \log(\text{O}/\text{H}) = 8.3$, and the one in the present investigation. The simplest explanation could be the low quality of the data here or the use of empirical method in Hunter & Hoffman. Besides, the oxygen abundance obtained with McGaugh's method is presented in the last row in Table 4, and the differences persist.

The other two galaxies (DDO 190 and IC 5152) present oxygen abundances similar to those found for another two dI previously investigated, NGC 6822 and IC 4662. Aparicio & Tikhonov (2000) derived a rather low iron abundance for DDO 190 from the $(V - I)$ color ($[\text{Fe}/\text{H}] = -2.00$). It should be mentioned that their value is obtained from fitting of model isochrones to the CMD, with larger inherent uncertainties than direct measurements of the abundance.

Concerning IC 5152, Zijlstra & Minniti (1999) obtained from colour-magnitude diagrams a very low metallicity ($Z = 0.002$). This value is lower than the one presented here. Note that their value is obtained by fitting model isochrones to the CMD, also. Some differences are found between the oxygen abundance of IC 5152 obtained in the present investigation, $12 + \log(\text{O}/\text{H}) = 8.2$, and these presented in Talent (1980), 8.36, and in Webster et al. (1983), 8.4, both very close to the LMC abundance. In Talent's and in the present investigation, the temperature sensitive method (Osterbrock 1989) was used for the determination of the T_e , but the determination made by Webster et al. was obtained with the aid of the so called semi-empirical method (Pagel et al. 1979). One should keep in mind that the abundances of IC 5152 derived in this work does not contain the main body of the galaxy, but one of those small H II regions described in Sect. 2.

5. Chemical evolution of gas-rich galaxies

It has been proposed that for low metallicity star forming galaxies, the abundance ratio $\log(\text{N}/\text{O})$ is constant around -1.5 , indicating a primary origin of nitrogen (Garnett 1990; Masegosa 1994; Izotov & Thuan 1999). This relation is presented in Fig. 1b for all the H II regions in all the dIs included in this analysis, as well as for NGC 6822 (Paper I), IC 4662, ESO 245-G05 (Paper II), DDO 50 and IC 10 (Hidalgo-Gómez 1999). The small linear regression coefficient ($r_1 = -0.48$) indicates that nitrogen is very much primary for these dI galaxies. As evident from this figure, two objects (ESO 245-G05 and IC 4662 D) show a strong deviation from the general trend. They present large values, closer to those of spiral galaxies. IC 4662 D shows a normal behaviour on the $12 + \log(\text{O}/\text{H})$ vs. $\log(\text{N}/\text{H})$ diagram (Fig. 1a) while ESO 245-G05 No. 12 has a real overabundance in nitrogen (for more details

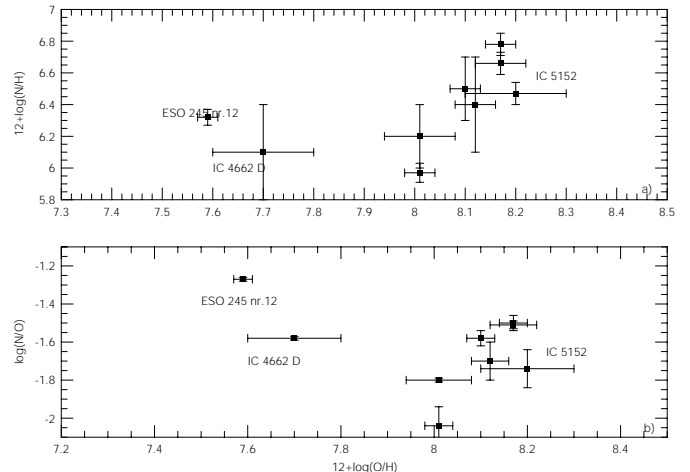


Fig. 1. **a)** The correlation between the nitrogen and oxygen abundance for the sample of dI galaxies. The linear regression coefficient is $r_1 = 0.51$ for a total of 8 data points. **b)** The $12 + \log(\text{O}/\text{H})$ vs. $\log(\text{N}/\text{O})$ plane for the same sample. The linear regression coefficient is -0.48 .

on the overabundances of this region, see Paper II). The general trend in Fig. 1b is very close to the predicted evolutionary tracks by Pilyugin (1992). The main difference is the larger values of $\log(\text{N}/\text{O})$ obtained from the model. Pilyugin (1992) used a closed-box model, which produce higher abundances than the observed (Pilyugin & Ferrini 2000; Hidalgo-Gómez et al. 2002).

Figure 2a presents the correlation between the oxygen and neon abundances for the sample of dI galaxies, which is strong ($r_1 = 0.82$) and support the idea that oxygen and neon are, basically, the product of the same type of stars. In Fig. 2b is visualized the relation between the oxygen abundance and the ratio $\log(\text{Ne}/\text{O})$. Due to the large uncertainties associated with the intensity of the neon lines, any conclusion should be treated with caution. However, the $\log(\text{Ne}/\text{O})$ ratio could be taken as constant around -0.7 , with a dispersion of $\sigma = 0.33$.

5.1. Comparison with other similar galaxies

Two important topics will be discussed in this section. The first one concerns the differences, if any, in the physical processes occurring inside H II regions with different strength of star formation. A second one is related with the proposed evolutionary connections between the different types of gas-rich galaxies (e.g. Davies & Phillips 1988).

In order to gain some insight into these topics, a comparison is made between the 12 H II regions in our dI sample and other gas-rich galaxies. The metallicity of all of the H II regions were obtained with the standard method.

The samples are the following: 28 H II regions in Blue Compact Galaxies (BCGs) (Izotov & Thuan 1999; Izotov et al. 1997; Izotov et al. 1994). A total of 17 dwarf Low Surface Brightness Galaxies (dLSBG) from the sample of van Zee et al. (1997). 13 H II regions in Low Surface

Table 4. Average chemical abundance and abundance ratios in H II regions of various types of star forming galaxies. Data have been taken from; dI: Paper I, Paper II and this investigation, BCG: Izotov & Thuan (1999), dLSBG: van Zee et al. (1997) LSBG: McGaugh (1994), Sp: McCall et al. (1985). The numbers in parenthesis are the dispersions of the sample, calculated as $\sigma^2 = \frac{1}{N}[(\sum x_i^2 - \frac{1}{N}(\sum x_i)^2)]$.

	dI	BCG	dLSBG	LSBG	Sp
[OIII]/[OII]	2.32	4.29	1.46	1.46	1.50
[OIII]/H β	3.91	4.65	3.28	3.28	3.56
$EW(H\beta)$	115 Å	120 Å	85 Å	45 Å	118 Å
$12 + \log(O/H)$	7.84 (.4)	7.90 (.3)	7.98 (.3)	7.80 (.5)	8.04 (.3)
$12 + \log(N/H)$	6.38 (.2)	6.40 (.4)	6.38 (.4)	6.28 (.3)	6.79 (.4)
$12 + \log(Ne/H)$	7.28 (.3)	7.22 (.4)	7.31 (.4)	7.55 (.5)	7.36 (.2)
$\log(N/O)$	-1.63 (.2)	-1.51 (.22)	-1.54 (.22)	-1.46 (.2)	-1.14 (.5)
$\log(Ne/O)$	-0.54 (.4)	-0.71 (.04)	-0.67 (.04)	-0.31 (.3)	-0.69 (.2)

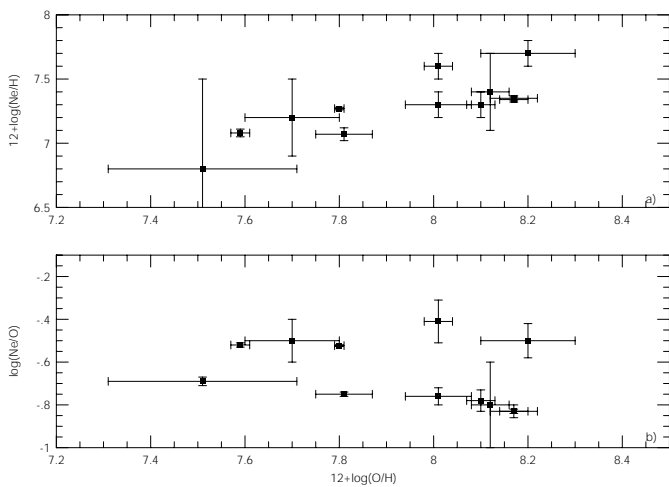


Fig. 2. a) The correlation between the neon and oxygen abundance for the sample of dI galaxies. The linear regression coefficient is $r_1 = 0.83$ for a total of 11 data points. **b)** The $12 + \log(O/H)$ vs. $\log(Ne/O)$ plane for the same sample, with $r_1 = -0.28$.

Brightness Galaxies (LSBGs) (McGaugh 1994) where the oxygen line [OIII] λ 4363 Å was observed. McGaugh only presented oxygen abundances in his sample but nitrogen and neon abundances were obtained by the authors with the same software used here. Information on 8 H II regions in a sample of spiral galaxies (Sp) from McCall et al. (1985) was added for comparison.

Gallagher & Hunter (1984) studied the differences between the H II regions in spiral and large irregular galaxies and they concluded that once the star formation is triggered the H II region forgets which kind of galaxy hosts it. In that sense, no differences could be found in colours, sizes and other characteristics. Recently, it has been claimed (Östlin, Masegosa, private communication) that H II regions in different types of gas-rich galaxies are not comparable, suffering different physical processes, especially BCG. Hidalgo-Gómez (1999) supported the idea of indistinguishable star formation regions for all the gas-rich type galaxies. The only difference between BCG and

the rest of the rich-gas might be the strength or the age of the star formation event.

Some information on the strength of the star formation event could be obtained from the excitation and the ionization parameters, defined as in Paper I. Their averaged values are presented in Table 4 for all the galaxies. A most complete information could be inferred not only from these numbers but also from their spatial distribution throughout the regions studied. Such study is out of the scope of this paper.

An important difficulty is the dependence of these parameters on the IMF and on the age of the star formation event as well as on the strength of the event. In the most likely situation different values might indicate differences either in the strength or in the IMF and the age. From the data of Table 4 very few conclusions could be obtained. However, the simplest approach is to consider a unique IMF for all this type of galaxies and trace the ages of the H II regions with the use of the equivalent width of the H β line. The conclusions could be outlined as following: The events in BCG and dI seem to be contemporary and the differences in the ionization and excitation should be explained in terms of the more powerful event in the BCG than in dI (e.g. large number of massive stars). The situation for the two samples of LSB galaxies is the opposite. They have very similar values of the excitation and ionization parameters, but very different times for the star formation. The main difference between spirals and BCG and dI is the ionization fraction but both the excitation and the equivalent width are very similar.

Many attempts have been done to obtain an evolutionary connection between the different types of gas-rich galaxies: LSBG, BCG and dI (Davies & Phillips 1988; Simpson & Gottesman 2000; van Zee et al. 2001; Masafumi 2001). In most of the cases, they focused on the colours, sizes, SFH and other parameter. Any evolutionary trend between all these galaxies or a subset of them should consider also the evolution of the metal content of them. A typical evolutionary scenario for gas-rich galaxies is (dLSBG \rightarrow) BCG \rightarrow dI \rightarrow dLSBG. Typically, the duration of the star formation events is about few hundreds Myr (Dohm-Palmer et al. 1998). In that case, a rising

trend in the oxygen and neon contents should be detected when going from the BCG to the dLSBG while the nitrogen should keep constant or slowly growing, due to the difference in the release time of these two elements, approximately 30 Myr (Recchi et al. 2001), and the partially secondary nature of this element.

In order to get some insights on the possible evolutionary trends, average values of the content of nitrogen, oxygen and neon are also presented in Table 4, as well as for the abundance ratios $\log(N/O)$ and $\log(Ne/O)$ for each set of data. Also, the dispersion for each set of data is presented. The first conclusion is that taking into account the large dispersion values the abundances of all the elements might be considered constant throughout the different subtypes of gas-rich galaxies. In any case, small differences in the chemical abundances are noticed among them. Nitrogen seems to be constant in the BCG, LSBG and dI, but neither the oxygen nor the neon follow the expected enhancement. The highest oxygen abundances are presented in the dLSBG and the lowest in the dI, with a difference of 0.14 dex. An interpretation of this behaviour could be with the use of (selective) galactic winds (e.g. Matteucci & Chiosi 1983). The oxygen is released from the galaxy due to, mainly, SN explosions. This scenario fits well with the data on Table 4. Between the BCG and the dI “phases” the SN explosions take place and most of the oxygen which is created by the massive stars is pushed away from the galaxy. The enhancement of the dLSBG could be explained from the oxygen created by less massive stars. An important problem might be the nearly constant value of the neon abundance, which is opposed to the expected result.

Another explanation for these small differences might be through the relationship between the gas-mass fraction and the metal content. This relationship follows the expression (Hidalgo-Gómez et al. 2002)

$$Z(\nu) = \left(Z' + \frac{y_z}{b} \right) (1 - \exp(-b\nu)) \quad (1)$$

for a particular model that includes infalls and outflows of gas. ν is the gas-mass fraction and y_z is the yield as defined by Tinsley (1980) and b is the ratio between the infalls (A) and outflows (W) of gas, $b = (A - W)/A$. Large values of the M_{HI}/L_B ratio increase the metallicity of the galaxies. Van Zee et al. (1997) obtained a slightly large value of this ratio for dLSBGs than the typical of dIs. In this sense, it can be concluded that the differences in the abundances among the dwarf galaxies might reflect differences in the gas-mass fraction, the environment or the dark matter content as discussed in Hidalgo-Gómez et al. (2002). Moreover, Recchi et al. (2001) simulated the ejection of enriched gas for dwarf gas-rich galaxies. The ejecta of metals is larger when the gas mass is smaller, which correspond to the dI and BDG. In addition, the metals are ejected in earlier times than in the case of more massive galaxies. Therefore it can be concluded that the large values of the M/L ratio and a large enrichment from

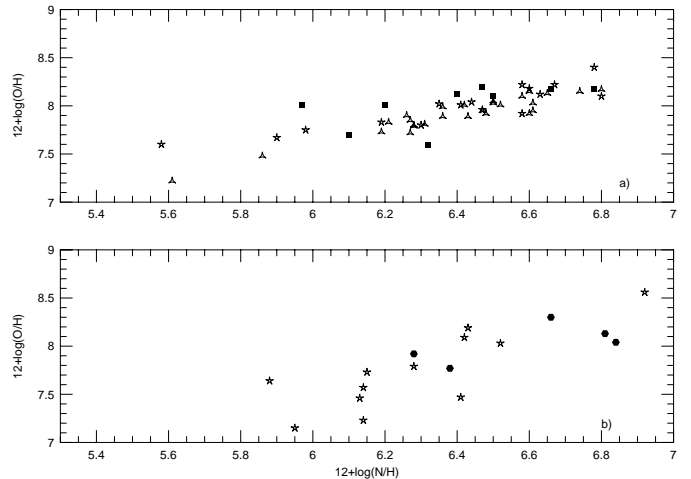


Fig. 3. The nitrogen vs. oxygen abundances for a sample of gas-rich galaxies. **a)** dI (filled squares), BCG (empty triangles) and dLSBG (empty stars). The dispersion is $\sigma = 0.25$. **b)** Sp (filled circles) and LSBG (stars). The dispersion for the large gas-rich galaxies is larger, $\sigma = 0.39$. The linear correlation coefficient for each type of galaxy is $r_1 = 0.55$ for dIs, 0.86 for BCGs, 0.82 for LSBGs and 0.41 for Sps.

SN explosions can account for the differences in the metal content of dLSBG.

The LSBG sample seem to have a different chemical evolution. The oxygen and nitrogen abundances are very low, the lowest values of the whole sample, but the neon is the highest. No evolutionary scenario could be fitted to these values. According to Eq. (1), those galaxies with small values of the ν parameter, defined as the ratio between the stellar and the gas mass, have small metallicities. For LSBG galaxies ν is small due to the large amount of gas and the small number of stars. Therefore, their metallicities can be explained because of the low ν values.

In order to go deeper into the differences and similarities between the different groups of gas-rich galaxies, each of the data points of the samples are presented in Figs. 3 to 6. Figure 3a presents the relationship between the nitrogen and oxygen content for the dLSB, BC and dI galaxies. The same relationship for LSBG and Sp is presented in Fig. 3b. The dwarf galaxies follow a very tight correlation ($r_1 = 0.8$) and they are indistinguishable in this plot. The dispersion of the three samples is $\sigma = 0.26$. For the LSBG and Sp samples a higher dispersion is observed ($\sigma = 0.4$), despite the similar regression coefficient ($r_1 = 0.7$). A clear separation could be established for them with the spirals at the top end, as expected.

Figure 4a is perhaps the most interesting. From this figures it is not so clear the claimed trend between the nitrogen and oxygen for high metallicities, which indicates a secondary origin for nitrogen. One possible reason is the small number of high metallicity objects. The same is also true for the large gas-rich sample (Sp and LSBG) showed in Fig. 4b. From Fig. 4a, a constant value of -1.6 with a σ of 0.2 could be determined for the $\log(N/O)$,

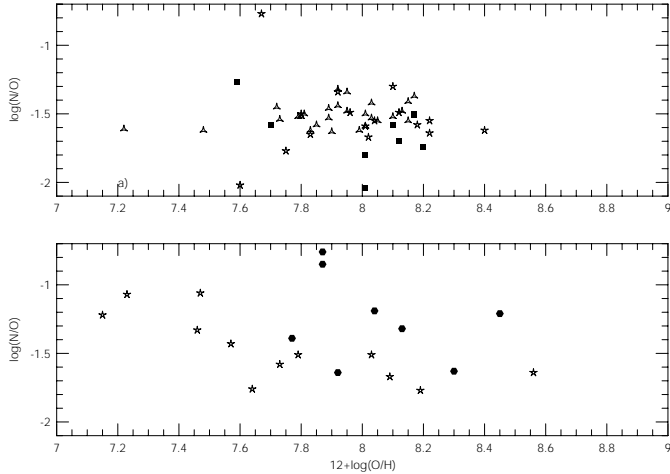


Fig. 4. The $12 + \log(\text{O}/\text{H})$ vs. $\log(\text{N}/\text{O})$ plane. Symbols are as in Fig. 3. The top of the figure correspond to the dwarf gas-rich galaxies and the lower part to the large gas-rich. The dispersions are 0.17 and 0.28, respectively. The linear correlation coefficients are $r_1 = -0.4$ for dIs, 0.38 for BCGs, -0.74 for LSBGs and -0.24 for Sps. The two data points corresponding to Sps at the top and the three data points of LBSG at the top-left may be erroneous to some extent.

which indicates a primary origin of nitrogen for all types of dwarf gas-rich galaxies. Again, the largest galaxies present a larger spread in their distribution, $\sigma = 0.5$, but the same tendency. The objects at the upper part of the diagrams should be considered erroneous due to high uncertainties.

Figure 5a shows the correlation between the oxygen and the neon content for dwarf gas-rich galaxies. Here, the correlation is also very tight ($r_1 = 0.8$) and indicates the common origin of these elements. The same is true for the large galaxies (Fig. 5b). Important differences appear when the relationship between the $\log(\text{Ne}/\text{O})$ and $12 + \log(\text{O}/\text{H})$ is considered (Figs. 7a and b). While for the dwarf galaxies a constant value on $\log(\text{Ne}/\text{O})$ of -0.7 could be inferred, the sample of large galaxies present a trend with the spiral galaxies located at the low right end. The dispersion are 0.09 and 0.24, respectively. Values larger than -0.2 should be considered erroneous to some extent.

From these figures it is clear that LSBG reveal a large spread over the whole diagrams. This may indicate that different morphological types of galaxies are classified as LSBGs. A similar conclusion can be drawn from a closer inspection of McGaugh's sample, where, preferably, large size galaxies were selected.

Some conclusions can be drawn from these comparisons. First, the sizes of the galaxies seems to play an important role on their chemical evolution. In this sense, distinction should be made between large and dwarf galaxies. Similar results to those presented here were found by Hunter & Hoffman (1999). They studied samples of dI, BCD and Sm galaxies and found that BCD and dI have the same metallicities and smaller values than the Sm galaxies. Secondly, and more important, from the chemical

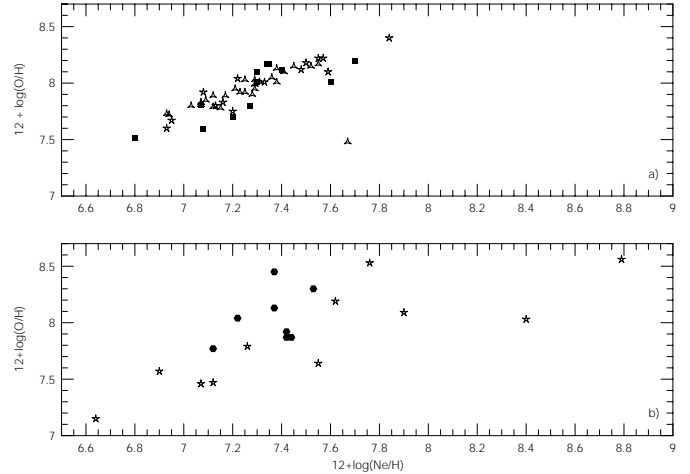


Fig. 5. The $12 + \log(\text{O}/\text{H})$ vs. $12 + \log(\text{Ne}/\text{H})$ plane. Symbols as in Fig. 3. Again, the top part of the figure are the dwarf and the low figure are the large gas-rich galaxies. Dispersions are 0.24 and 0.5 respectively. The linear correlation coefficients are $r_1 = 0.81$ for dIs, 0.72 for BCGs, 0.84 for LSBGs and 0.38 for Sps.

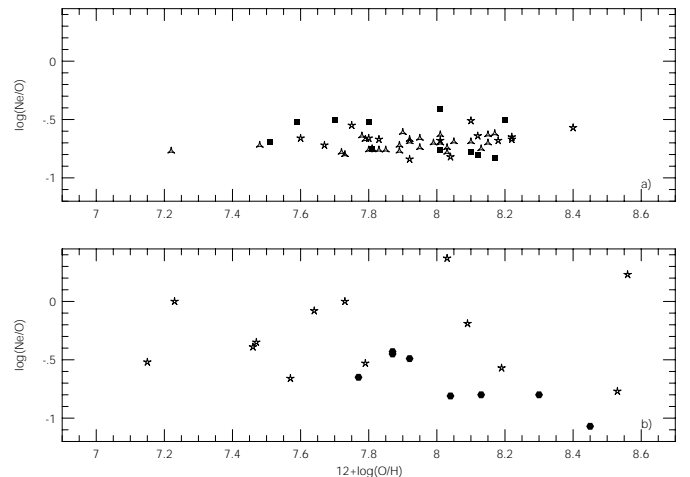


Fig. 6. The $12 + \log(\text{O}/\text{H})$ vs. $\log(\text{Ne}/\text{O})$ plane. Symbols as in Figure 3. The dispersion for the dwarf galaxies, **a**), is 0.1 and for the large **b**) is 9.3. The linear correlation coefficients are $r_1 = 0.36$ for dIs, 0.4 for BCG, 0.23 for LSBGs and -0.85 for Sps.

content no distinction is clear between the dwarf galaxies group. From Figs. 3 to 6, it could be concluded that dwarf gas-rich galaxies shared the same locii in all the planes and there is not any systematic differences for any of the groups, e.g. being always at the lowest or the highest ends. It must be concluded that galaxies with very low metallicity are dwarf gas-rich, but these do not belong to any specific group defined on the basis of their optical surface brightness.

6. Conclusions

Abundances of nitrogen, oxygen and neon of five nearby dIs have been derived. The abundances were found to be sub-solar in all cases. For the dwarf irregular galaxy

DDO 190 the abundances reported in this work are the first ones ever published. The H II region observed in IC 5152 might contain a SN type II or a WR star. From the spectral characteristic studied in the present investigation they could not be distinguished. Three of the galaxies present very low oxygen abundances with large uncertainties. New observations will be very helpful in order to decrease the uncertainties.

A comparison with other types or gas-rich galaxies indicates that the physical processes taking place in the objects are the same and the only difference is the strength of the star-forming event. Considering an evolutionary scenario, a sequence like the following: dLSBG, BCG and dI could be well explained considering selective winds or with the differences in the gas-mass fraction. On the other hand, large LSBG could not be related to BCG or dI when element abundances are taken into account.

Acknowledgements. The authors want to thanks J.-R. Roy for many useful comments which improved this paper and F. J. Sánchez-Salcedo for a carefully reading of the manuscript. The referee, J. Gallagher, is thanked for many comments which improved the manuscript. P. Leisy, D. Polanco, G. Reis, H. Scharwz and A. Pharasyn are indebted for their help. N. Bergvall is thanked for supplying and updating a new version of his software. A.M.H.G. had been financially supported by NOTSA and by UAO. A.M.H.G. thanks the Instituto de Astronomía-UNAM for their hospitality and to L. Binette for support through CONACyT grant 32139-E.

References

- Aller, L. H. 1984, *Physics of Gaseous Nebulae* (Reidel Publishing Co., Dordrech)
- Aparicio, A., & Tikhonov, N. 2000, *AJ*, 119, 2183
- Davies, J. I., & Phillips, S. 1989, *Ap&SS*, 157, 291
- Dohm-Palmer, R., Skillman, E. D., Gallagher, J., et al. 1998, *AJ*, 116, 1227
- Gallagher, J. S. III, & Hunter, D. A. 1984, *ARA&A*, 22, 37
- Gallagher, J. S. III, & Hunter, D. A. 1986, *AJ*, 92, 557
- Garnett, D. 1990, *ApJ*, 363, 142
- Hidalgo-Gómez, A. M. 1999, Ph.D. Thesis, Uppsala University
- Hidalgo-Gómez, A. M., & Olofsson, K. 1998, *A&A*, 334, 45 (HGO)
- Hidalgo-Gómez, A. M., Olofsson, K., & Masegosa, J. 2001, *A&A*, 367, 388 (Paper I)
- Hidalgo-Gómez, A. M., Masegosa, J., & Olofsson, K. 2001, *A&A*, 369 (Paper II)
- Hidalgo-Gómez, A. M., Sánchez-Salcedo, F. J., & Olofsson, K. 2002, *A&A*, submitted
- Hunter, D. A., & Gallagher, J. S. III 1985, *ApJS*, 58, 533
- Hunter, D. A., & Hoffman, L. 1999, *AJ*, 117, 2789
- Izotov, Y. I., Thuan, T. X., & Lipovetsky, V. A. 1994, *ApJ*, 435, 647
- Izotov, Y. I., Thuan, T. X., & Lipovetsky, V. A. 1997, *ApJS*, 108, 1
- Izotov, Y. I., & Thuan, T. X. 1999, *ApJ*, 511, 639
- Kennicutt, R. C. Jr., Edgar, B. K., & Hodge, P. W. 1989, *ApJ*, 337, 761
- Kunth, D., & Sargent, W. L. W. 1986, *ApJ*, 300, 496
- Masafumi, N. 2001, *ApJ*, 555, 289
- Masegosa, J. 1988, Ph.D. Thesis, Universidad de Granada
- Masegosa, J., Moles, M., & Campos-Aguilar, A. 1994, *ApJ*, 420, 576
- Matteucci, F., & Chiosi, C. 1983, *A&A*, 123, 121
- McCall, M. L., Rybski, P. M., & Shields, G. A. 1985, *ApJS*, 57, 1
- McGaugh, S. S. 1994, *ApJ*, 426, 135
- Melisse, J. P. M., & Israel, F. P. 1994, *A&A*, 285, 51
- Moles, M., Aparicio, A., & Masegosa, J. 1990, *A&A*, 228, 310
- Olofsson, K. 1997, *A&A*, 321, 29
- Osterbrock, D. E. 1989, *Astrophysics of Gaseous Nebulae and Active Galactic Nuclei* (University Science Books, Mill Valley, CA)
- Pagel, B. E. J., Edmunds, M. G., Blackwell, D. E., et al. 1979, *MNRAS*, 189, 95
- Pilyugin, L. S. 1992, *A&A*, 260, 58
- Pilyugin, L. S., & Ferrini, F. 2000, *A&A*, 358, 72
- Recchi, S., Matteucci, F., & D'Ercole, A. 2001, *MNRAS*, 322, 800
- Schulte-Ladbeck, R. E., & Hopp, E. 1998, *AJ*, 116, 2886
- Simpson, C. E., & Gottesman, S. T. 2000, *AJ*, 120, 2975
- Skillman, E. D., Melnick, J., Terlevich, R., & Moles, M. 1988, *A&A*, 196, 31
- Skillman, E. D. 1989, *ApJ*, 347, 883
- Skillman, E. D., Kennicutt, R. C. Jr., & Hodge, P. 1989, *ApJ*, 347, 875
- Stasińska, G. 1990, *A&AS*, 83, 501
- Strobel, N. V., Hodge, P., & Kennicutt, R. C. Jr. 1991, *ApJ*, 383, 148
- Talent, D. L. 1980, Ph.D. Thesis, University of Rice
- de Vaucouleurs, G., de Vaucouleurs, A., Corwin, H. G., et al. 1991, *Third Reference Catalogue of Bright Galaxies* (Springer-Verlag)
- van den Bergh, S. 1966, *AJ*, 71, 922
- van Zee, L., Salzer, J., & Skillman, E. D. 2001, *AJ*, 122, 121
- Webster, B. L., Longmore, A. J., Hawarden, T. G., & Mebold, U. 1983, *MNRAS*, 205, 643
- Zijlstra, A. A., & Minniti, D. 1999, *AJ*, 117, 1743